SPECTROPOLARIMETRY OF THE LUMINOUS NARROW-LINE SEYFERT GALAXIES IRAS 20181−2244 AND IRAS 13224−3809

Laura E. Kay[1,2]

Department of Physics and Astronomy, Barnard College, Columbia University, New York, NY 10027

AND

A. M. Magalhães,[1,4] F. Elizalde,[3,4] and C. Rodrigues[3]

Instituto Astronômico e Geofísico, Universidade de São Paulo, Caixa Postal 3386, São Paulo, SP 01060-970, Brazil

ABSTRACT

We observed the narrow-line Seyfert 1 galaxies IRAS 20181−2244 and IRAS 13224−3809 with a new spectropolarimeter on the Ritchey-Chrétien spectrograph at the CTIO 4 m telescope. Previously it had been suggested that IRAS 20181−2244 was a type 2 QSO and thus might contain an obscured broad-line region that could be detected by the presence of broad Balmer lines in the polarized flux. We found the object to be polarized at about 2% and constant with wavelength (unlike most narrow-line Seyfert 1 galaxies), but with no evidence of broad Balmer lines in polarized flux. The spectropolarimetry indicates that the scattering material is inside the broad-line region. IRAS 13224−3809, notable for its high variability in X-ray and UV wavelengths, has a low polarization consistent with a Galactic interstellar origin.

Subject headings: galaxies: active — galaxies: individual (IRAS 20181−2244, IRAS 13224−3809) — galaxies: Seyfert — polarization

1. INTRODUCTION

IRAS 20181−2244 and IRAS 13224−3809 are part of the Boller et al. (1992) sample of bright *IRAS* galaxies, which were also identified as soft X-ray sources by *ROSAT*. Elizalde & Steiner (1994) reported that IRAS 20181−2244 has a Seyfert 2–type spectrum and an absolute magnitude bright enough to be called a QSO, and they suggested that it qualifies as one of the elusive type 2 (narrow-line) QSOs.

Previous studies have shown that some type 2 active galactic nuclei (AGNs), with narrow permitted and forbidden emission lines, have obscured broad-line regions (BLRs) that are visible only in reflected and scattered—and thus polarized—light. Thus the polarized flux of these obscured type 2 objects have broad Balmer lines, i.e., they look like the total flux of a type 1 object with broad permitted and narrow forbidden lines. This has been seen for about 12 "classical" Seyfert 2 galaxies, some narrow-line radio galaxies, and about a half-dozen narrow-line ultraluminous *IRAS* galaxies with luminosities comparable to those of QSOs (see, e.g., Antonucci & Miller 1985; Miller & Goodrich 1990; Kay, Antonucci, & Coleman 1992; Tran, Cohen, & Goodrich 1995; Young et al. 1996; Heisler et al. 1997; Kay & Moran 1998). In QSOs, the AGNs with the highest luminosities, only the type 1 broad-line objects normally are seen. If QSOs are to fit into these "unified models" of AGNs, we should be observing some of them also at an orientation in which the BLR is obscured, so that they appear as very luminous objects with only narrow emission lines in their spectra.

There have been numerous transitory claims of observations of such type 2 QSOs, especially in X-ray–identified targets, usually because their optical spectra were of low signal-to-noise ratio (S/N) or because they did not include the Hα spectral region. Indeed, in their optical survey of the northern Boller et al. (1992) sample, Moran, Helfand, & Halpern (1996) reclassified IRAS 20181−2244 as a narrow-line Seyfert 1 (NLS1). These Seyfert galaxies were first identified by Phillips (1976) and Osterbrock & Pogge (1985) and are sometimes called I Zw 1 objects after their prototype. These objects have narrow forbidden and permitted lines, high-ionization lines as in classical Seyfert 2 galaxies, strong permitted narrow Fe II emission-line complexes, and usually an [O III] $\lambda5007$ to Hβ flux ratio less than 3. A comprehensive analysis of their 1994 optical spectra of IRAS 20181−2244 confirmed their initial reclassification (Halpern & Moran 1998). NLS1s often are highly represented in soft X-ray–selected samples (Stephens 1989; Moran et al. 1996), and thus this classification is not surprising.

We observed IRAS 20181−2244 ($z = 0.185$) in order to look for a possible obscured BLR, as indicated by broad Hα and Hβ emission lines in polarized flux and to see how its polarization properties compared with other similar targets. We present spectropolarimetry of this AGN, taken at the CTIO 4 m telescope with a visitor polarimetry unit on the Ritchey-Chrétien spectrograph, and imaging polarimetry from the Laboratório Nacional de Astrofísica (LNA) 1.6 m telescope in Brasópolis. Another narrow-line Seyfert 1 galaxy, IRAS 13224−3809 ($z = 0.067$), was also observed with spectropolarimetry.

---

[1] Visiting Astronomer, Cerro Tololo Inter-American Observatory. CTIO is operated by AURA, Inc., under contract to the National Science Foundation.

[2] NSF International Research Fellow, IAG-USP.

[3] Present address: INPE-DAS, Caixa Postal 515, São Jose dos Campos, SP 12201-970, Brazil.

[4] Visiting Astronomer, CNPq/Laboratório Nacional de Astrofísica.

2. OBSERVATIONS AND DATA REDUCTION

2.1. *Spectropolarimetry*

These observations took place during the first test run of the CTIO spectropolarimeter on 1995 May 23. We used the Ritchey-Chrétien spectrograph at the CTIO 4 m telescope

TABLE 1
CTIO SPECTROPOLARIMETRY OBSERVATIONS

Object	Date (UT)	Exposure (minutes)	P (%)	σ_P (%)	θ (deg)
IRAS 20181−2244......	1995 May 23	120	1.86	0.07	131 ± 1
IRAS 13224−3809......	1995 May 23	60	0.38	0.03	84 ± 2

with a Loral 3k CCD, a KPGL3 grating with a dispersion of 1.2 Å pixel^{-1}, a spectral resolution of 4 Å, and a wavelength range of 4445–8150 Å. Additional optics were placed into the spectrograph in order to conduct the polarimetry observations. A rotatable superachromatic half-wave plate (Frecker & Serkowski 1974) with 19 mm clear aperture (manufactured by Halle in Germany) was installed 63 mm above the slit. The wave plate was rotated in 22°.5 steps with an external controller built at the University of Wisconsin. Miller, Robinson, & Goodrich (1988) discuss the advantages of a dual-beam instrument for spectropolarimetry. For a beamsplitting device we used a 44 mm diameter square double calcite block (Savart plate, built at Optoeletrônica, São Paulo), which was mounted 78 mm below the slit. Each component prism was cut with its optical axis at 45° to its face, and they were cemented with their optical axes crossed. This arrangement minimizes the astigmatism and color that are present when a single calcite block is used (Serkowski 1974). This beamsplitter produces two spectra of the given object, separated by 1 mm and with orthogonal polarizations. A comb decker used for observations had a series of parallel slots each about 1 mm wide. This system is more similar to the spectropolarimeter on the ISIS spectrograph at the William Herschel Telescope (WHT; Tinbergen & Rutten 1992) than to the instruments recently constructed in the US (see, e.g., Goodrich 1991). An advantage of using a Savart plate is that the focus of the two beams is consistent, and a disadvantage is that the length of the slit with the comb decker is short.

We tested the instrumental polarization by observing the published null standard stars HD 100623 and HD 98161 at all 16 positions of the wave plate. Even though images at only four consecutive positions of the wave plate (e.g., 0°–67°.5) are needed for a polarization measurement, observation at all available positions allows the overall performance of the polarimeter, in particular the residuals at each position angle, to be inspected. The linear polarization P measured for these objects was 0.03% or less. Polarization standard stars HD 298383, HD 187929, HD 110984, and HD 155197 were also observed and were found to agree with published V-band values (Turnshek et al. 1990). The polarizance (the instrumental response to 100% polarized light) was found to be 98%. The zero point of the position angle correction curve, which depends on the position of the fast axis of the wave plate and the orientation of the beamsplitter, was obtained by comparing the measured polarization position angles of the standard stars with the published values. Spectropolarimetry data reduction and analysis were performed with the VISTA software package, originally developed at Lick Observatory, and additional routines.

IRAS 20181−2244 was observed for 15 minutes in each of eight wave-plate positions (0°–67°.5 and 180°–247°.5) for a total of 16 spectra in 2 hr. IRAS 13224−3809 was observed for 15 minutes in each of four wave-plate positions for a

total of eight spectra in 1 hr. Data were reduced following Miller et al. (1988), and all summing and averaging was done with the Stokes parameters Q and U. The averaged Q and U Stokes parameter spectra were used to create the observed polarizations presented in Table 1.

2.2. Imaging Polarimetry Observations

IRAS 20181−2244 was observed with a CCD imaging polarimeter (Magalhães et al. 1996) at the 1.6 m telescope at the LNA on 1994 September 1. These data are important to serve as a check on the spectropolarimetry measurements with a new system and to provide field stars for estimating the Galactic foreground polarization. The polarimeter is a modification of the observatory's direct CCD camera to allow for high precision imaging polarimetry. The first element in the beam is a rotatable, achromatic half-wave retarder followed by a Savart plate from the Instituto Astronômico e Geofisíco, University of São Paulo. This Savart plate was built similarly to the one used at CTIO. This gives us two images of each object in the field, separated by 1 mm (corresponding to about 13″ at the telescope focal plane) and with orthogonal polarizations. One polarization modulation cycle is covered for every 90° rotation of the wave plate. The simultaneous observations of the two beams allows observing under nonphotometric conditions at the same time that the sky polarization is practically canceled (Magalhães et al. 1996).

CCD exposures were taken through the V filter with the wave plate rotated through 12 positions 22°.5 apart. The exposure time at each position was 900 s. After bias and flat-field corrections, photometry was performed on the images of objects in the field with IRAF, and then a special-purpose FORTRAN routine processed these data files and calculated the normalized linear polarization from a least-squares solution. This yields the Stokes parameters Q and U, as well as the theoretical (i.e., photon noise) and measurement errors. The latter are obtained from the residuals of the observations at each wave-plate position angle (ψ_i) with regard to the expected $\cos 4\psi_i$ curve and are quoted in Table 2; they are consistent with the photon noise errors (Magalhães, Benedetti, & Roland 1984). The instrumental Q and U values were converted to the equatorial system from standard star data obtained in the same night. The instrumental polarization was measured to be less than 0.03%.

Figure 1 shows the field and identifies the objects. The separation between each pair of images is 1 mm, or 12″.9 at the 1.6 m f/10 LNA telescope. The size of the field shown in the image is 3′.7 × 5′.6. As noted in Moran et al. (1996) and shown in Figure 1 of Halpern & Moran (1998), IRAS 20181−2244 (object 1 in Fig. 1) is the extended object in the center of the field; object 2 is the one incorrectly identified instead in Figure 1 of Elizalde & Steiner (1994). The imaging polarimetry includes data on targets angularly close to the object of interest, thereby providing the means

TABLE 2

IMAGING POLARIZATION DATA FOR IRAS 20181−2244
AND FIELD STARS

Object	P (%)	σ_P (%)	θ (deg)
IRAS 20181−2244......	1.701	0.162	126.4
Field stars:			
2........................	0.487	0.126	12.1
3........................	0.478	0.119	22.4
4........................	0.803	0.206	25.1
5........................	0.468	0.124	24.8
6........................	0.596	0.177	16.6
7........................	0.561	0.169	20.0
Weighted average	0.520	0.059	20.2

to estimate the interstellar polarization toward a given direction.

Table 2 includes the polarization data for IRAS 20181−2244 and for six other objects in the field. For each target, the table gives the percent polarization, its error, and the equatorial position angle. The polarization values in Table 2 have not been corrected for statistical bias. IRAS 20181−2244 is more polarized than the other objects in the
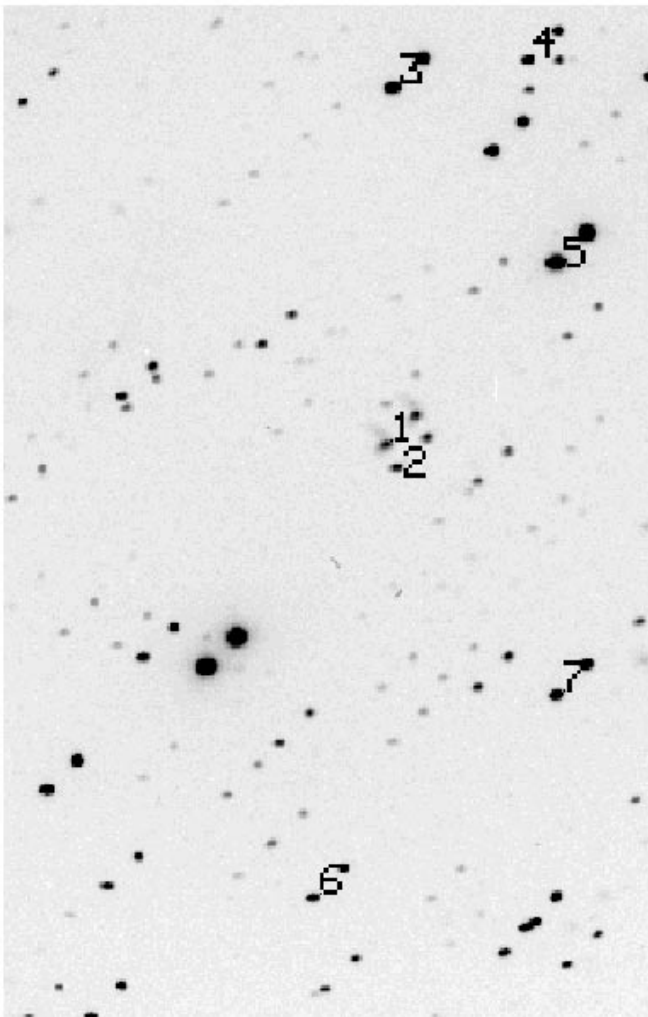
field, at $P = 1.70\% \pm 0.16\%$ and position angle 126°. The six field objects included in Table 2 were the ones that showed a (debiased) polarization larger than 3 σ. A weighted average, performed on the Stokes parameters of the field objects, yields a polarization of 0.520% ± 0.059% at 20°.2. The error of this estimate is entirely consistent with the average value of the individual measurement errors in Table 2 divided by $6^{1/2}$ (0.062%), as well as with the variance obtained from the spread of the individual Q and U values. We therefore take the average polarization value above as the Galactic foreground polarization toward IRAS 20181−2244. These values were used to correct the spectropolarimetry Stokes parameters Q and U.

3. RESULTS

3.1. *IRAS 20181−2244*

Figure 2 shows part of our deredshifted flux spectrum of IRAS 20181−2244. Measurements and analysis of the Balmer and forbidden lines were recently presented in Halpern & Moran (1998). We note that our higher S/N spectrum indicates broader wings on the Balmer lines than were seen in the spectrum of Elizalde & Steiner (1994), and the Fe II emission-line complexes discussed in Halpern & Moran (1998) are seen at 4500–4680 Å and 5105–5395 Å. Thus we concur with the classification of this object by the latter as a narrow-line Seyfert 1.

Figure 3 shows our spectropolarimetric observations of IRAS 20181−2244. The panels indicate the direct flux spectrum, the polarization (strictly, the rotated Stokes parameter, or RSP, obtained from rotating the Stokes Q and U by the average position angle θ: RSP = $Q \cos 2\theta + U \sin 2\theta$), the position angle of polarization, and the corresponding polarized flux (Stokes flux = RSP × flux). The polarization spectrum uncorrected for Galactic interstellar polarization shows an average P for $\lambda\lambda 5000$–6000 of about 1.72% ± 0.07%, at a position angle of 130° ± 1°, in excellent agreement with the imaging polarimetry measurement. When corrected for the Galactic interstellar polarization value in Table 2, we find P of about 2.3% ± 0.09% at $\theta = 127°$. The interstellar correction did not alter the original spectral shapes of the data in Figure 3. We have not

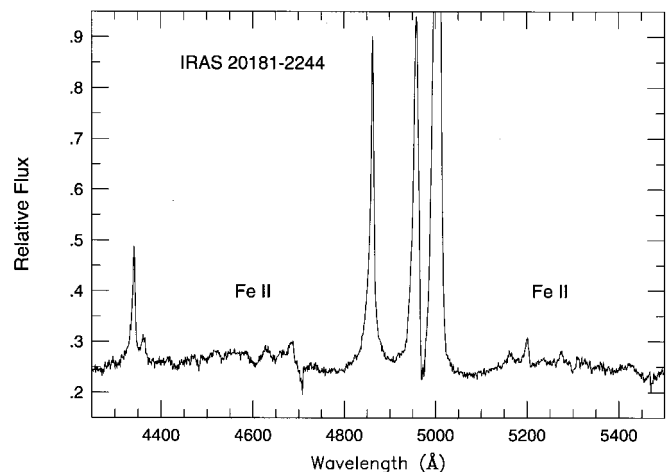FIG. 1.—Imaging polarimetry field for IRAS 20181−2244. Polarization data for the numbered stars is given in Table 2.

FIG. 2.—Spectroscopy of IRAS 20181−2244, showing the Fe II lines. The spectrum is not corrected for reddening. The flux is in units of 10^{-15} ergs s^{-1} cm^{-2} Å^{-1}.
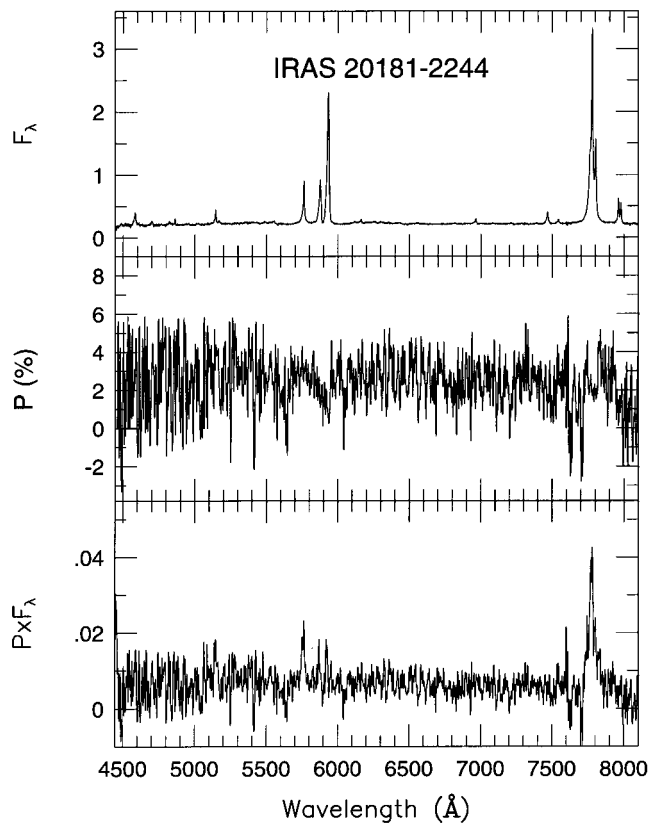
FIG. 3.—Spectropolarimetry of IRAS 20181−2244. The flux spectrum has units as in Fig. 2 and is not corrected for reddening or redshift. *Middle panel:* Polarization (RSP). *Bottom panel:* Corresponding polarized flux (the Stokes flux). The polarization and polarized flux spectra are corrected for the foreground Galactic polarization from Table 2, but are not completely corrected for 10 bad CCD columns on the blue wing of Hα or for the atmospheric bands.

corrected for starlight dilution of the polarization because we see no stellar absorption lines in the spectrum.

P is generally constant with wavelength and does not show the rise to the blue indicative of dust reflection as seen in the polarized narrow-line Seyfert 1 galaxies of Goodrich (1989). P may drop lower to near zero at the positions of the forbidden lines of [O III], which suggests these lines come from a spatially different nuclear region than Hα and Hβ. The position angle of polarization is constant, except for a rotation across the [O III] lines, indicating perhaps a separate source of polarization (e.g., transmission through dust grains in the host galaxy). IRAS 20181−2244 is detected as an unresolved 25 mJy source in the 20 cm NOAO VLA Sky Survey (Condon et al. 1998). A higher resolution radio observation of IRAS 20181−2244 with a good radio position angle is not yet available; thus we cannot compare radio and polarization position angles to see if they are perpendicular as in most Seyfert 2 galaxies (Antonucci 1983; Brindle et al. 1990), some NLS1s (Ulvestad, Antonucci, & Goodrich 1995), and some Seyfert 1 galaxies (Goodrich & Miller 1994), or parallel as in most Seyfert 1 galaxies (Antonucci 1983; Martel 1996). This comparison would be interesting, since there is considerable discussion as to whether NLS1s as a class are objects in which we are viewing the disk pole-on (see, e.g., Osterbrock & Pogge 1985; Puchnarewicz et al. 1992; Ulvestad et al. 1995). The relatively high P value we obtained would argue

against this, although it may be produced by scatterers symmetrically distributed around the central source.

In the plot of the polarized flux, which shows the spectrum of the polarized light from the object, Hβ and Hα are visible, but the data are too noisy to measure an Hα/Hβ ratio accurately. The slopes of the continua in the direct and polarized flux spectra are both nearly flat. Figure 4 shows the Hβ line profile in flux (*heavy line*) and polarized flux. The FWHM of Hβ in both direct and polarized flux is about 600 km s^{-1}. Direct flux and polarized flux Hα also have a similar FWHM. The lines are not shifted in the polarized flux with respect to the direct flux. Thus the Balmer lines do not appear to be significantly broader in the polarized flux as we might expect if an obscured BLR was present and visible only in dust-scattered or electron-scattered—and thus polarized—light.

3.2. *IRAS 13224−3809*

The optical spectrum of the NLS1 IRAS 13224−3809 is discussed in Boller et al. (1993), who present line measurements, including the strong Fe II lines, and an Hα/Hβ ratio of 7.6. Figure 5 shows our spectropolarimetric observations of IRAS 13224−3809. The panels indicate the direct flux spectrum and the Q and U Stokes parameters. The average P is ∼0.38% at position angle 84°. We do not have imaging polarimetry of the field around IRAS 13224−3809, but given that it has a Galactic latitude of +24°, it would seem likely that some of this is attributable to Galactic interstellar polarization.

Mathewson & Ford (1970) include measurements of four stars (HD 114981, HD 116413, HD 117440, and HD 117597) that are within 3° of IRAS 13224−3809 in the sky. The polarizations and position angles of the polarization vary from 0.14% to 0.20% at 20°3–67°0, with the closest of these, HD 117597, 1°66 away in the sky, having the highest values. These stars are not all that close to the target, but it suggests that perhaps at least 0.2% of the measured polarization originates in the Galaxy. The Galactic $E(B-V)$ has been estimated from the distributed *IRAS* maps of Schlegel, Finkbeiner, & Davis (1998) as 0.12 mag. A similar estimate comes from using the Stark et al. (1992) neutral hydrogen column density $N_H = 7.3 \times 10^{20}$ cm^{-2}. Using $P_{max} \le 0.09E(B-V)$ (Serkowski, Mathewson, & Ford 1975), this suggests a maximum polarization from our
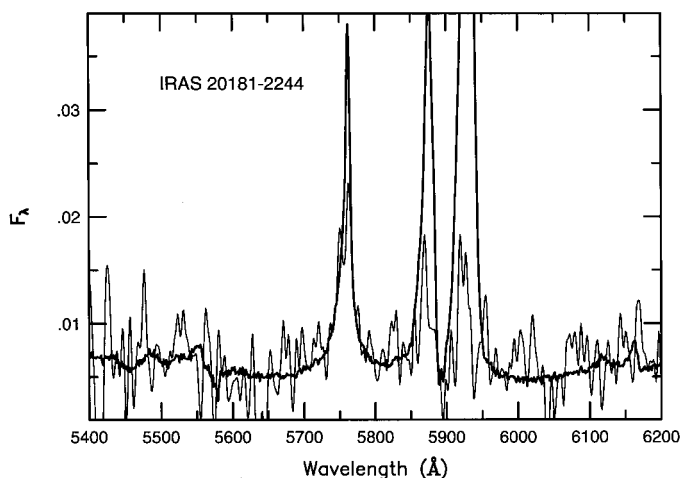

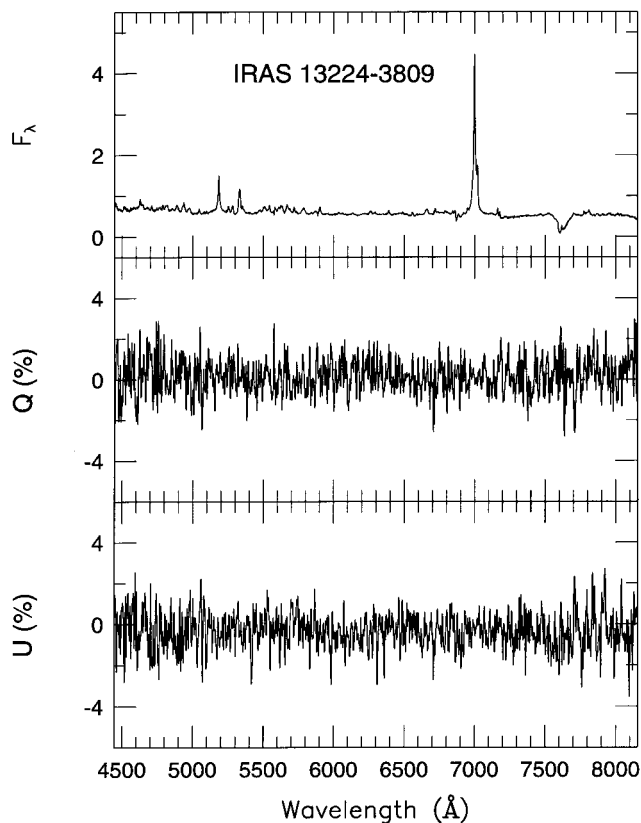FIG. 4.—Comparison of Hβ in direct (*heavy line*) and polarized flux for IRAS 20181−2244.

FIG. 5.—Spectropolarimetry of IRAS 13224−3809. *Top to bottom:* A flux spectrum as in the other figures, and Stokes *Q* and *U*, since *P* is so low.

Galaxy of 1.08%. However, the high Hα/Hβ ratio in IRAS 13224−3809 could indicate reddening and a possible dust transmission polarization component within the host galaxy.

4. DISCUSSION

4.1. *Continuum Polarization*

Many Seyfert 1 galaxies have a continuum polarization rising to the blue (see, e.g., Goodrich & Miller 1994; Martel 1996). Dust scattering is the most commonly suggested mechanism for this polarization, as the scattering cross section of small dust grains increases slowly toward shorter wavelengths. With the addition of redder nuclear light, the observed increase in polarization toward the blue steepens. The polarization of the NLS1 galaxies discussed in Goodrich (1989), as well as Mrk 486 (Smith et al. 1997) and IRAS 17020+4544 (Leighly et al. 1997), are attributed to dust scattering.

In general, polarized synchrotron radiation is insufficient to explain the observations because at least some of the lines are observed to be polarized. Polarization from dust transmission in our Galaxy or the host galaxy is nearly constant over 4000–7000 Å, but with a peak that corresponds to the grain size and a decrease toward smaller and larger wavelengths. The polarized flux would appear reddened (Goodrich 1989). Electron scattering will preserve the shape of the scattered spectrum, except possibly for a broadening of the Balmer lines in the polarized flux (unless the electrons are cool; even a relatively low electron temperature of 5000 K would broaden the line by 900 km s^{-1}, which would be noticeable in Fig. 4). However, electron

scattering combined with an unpolarized reddened nuclear light or redder starlight can also yield a continuum polarization that rises to the blue.

For example, Wills et al. (1992) observed IRAS 13349+2438, a luminous QSO with properties similar to an NLS1, and concluded that the wavelength dependence of its high polarization that rises to the blue is attributable to electron scattering, as well as to a dilution of the polarization by direct, unpolarized light from the reddened continuum. Smith et al. (1997) observed I Zw 1 with ground-based and *Hubble Space Telescope* (*HST*) spectropolarimetry, and found that the optical polarization was low but possibly time variable. They concluded that the wavelength dependence of the polarization of I Zw 1 is largely due to starlight from the host galaxy. When a correction was made for this, the continuum polarization became almost independent of wavelength from the UV to the red, and thus was likely due to scattering by electrons. This example indicates that unpolarized starlight can affect the polarization measurements even in an NLS1, and that it is possible that the polarization may change in some of these objects.

In our data of IRAS 20181−2244, the continuum polarization is nearly constant with wavelength (although the data do not go as far to the blue as in the objects discussed above). As noted by Goodrich (1989), it is difficult to estimate the starlight contribution to the direct flux spectrum because the Fe II emission lines contaminate the Mg I *b* and G-band stellar features. (Smith et al. 1997 derived a host galaxy spectrum for I Zw 1 using the total *H* magnitude of the host galaxy to estimate a galaxy fraction of 0.5 at 5500 Å, an unusually high starlight correction for a high-luminosity Seyfert 1.) We do not make a correction for starlight in the spectrum of IRAS 20181−2244, and thus find that it may have a similar continuum polarization to I Zw 1 due to electron scattering with a possible dust transmission component. Dust scattering seems less likely because the reddened continuum would steepen the rise toward the blue.

The polarization of IRAS 13224−3809 measured in our single set of observations is low enough to be consistent with a Galactic interstellar origin. Low polarization of NLS1s is not unusual; Goodrich (1989) found 11/17 of his NLS1s to be polarized at a level consistent with interstellar polarization from our Galaxy. Grupe et al. (1998) observed a sample of 43 bright soft X-ray–selected (*ROSAT*) AGNs, half of which were NLS1s, and found that only two NLS1s were polarized (IRAS 13349+2438 again, and IRAS F12397+3333). Another X-ray NLS1 galaxy with a similar spectrum to IRAS 13224−3809, which was found to be unpolarized (i.e., less than 0.4%), is RE J1034+396 (Puchnarewicz et al. 1995; Breeveld & Puchnarewicz 1998). The authors suggest this could be due to geometrical effects (symmetric distribution of scatterers so that the polarization vectors cancel out, e.g., as in a pole-on view), dilution of the polarization as proposed for IRAS 13349+2438 (Wills et al. 1992), or the absence of aligned dust grains in the line of sight. However, Boller et al. (1997) propose that an edge-on model, with a highly inclined inner accretion disk, can explain the strong X-ray variability and the soft X-ray excess of IRAS 13224−3809.

4.2. *Location of the Polarizing Material*

In the other polarized NLS1s (see, e.g., Goodrich 1989; Leighly et al. 1997), it is also generally found that the

narrow forbidden lines are less polarized than the Balmer lines, which can have a different polarization than the continuum. This suggests that the scattering material responsible for the observed polarization is between the narrow-line region and the BLR. The position angle does not vary across the Balmer lines; thus the scatterers are not likely within the BLR itself.

Recently Leighly et al. (1997) investigated the connection between optical polarization and the presence of warm absorber features in the X-ray spectra of a sample of Seyfert 1 galaxies. They showed that objects with optical polarizations greater than 1% are likely to have warm absorbers and suggested that this indicates a link between the warm absorber, reddened spectrum, and polarization. For example, the polarized NLS1 IRAS 17024+4544 contains a warm absorber as seen in the *ASCA* data (Leighly et al. 1997). Mrk 766, one of the three polarized NLS1 galaxies in Goodrich (1989), also has a warm absorber (Leighly et al. 1996). The *ASCA* X-ray spectrum of IRAS 20181−2244 has a neutral column density of $N_H = 1.6 \times 10^{21}$ cm^{-2} (Halpern & Moran 1998). Reanalysis shows that there is marginal evidence for a warm absorber (at the 95% confidence level; Leighly 1999). If the polarization indeed occurs inside the narrow-line region, this suggests that the absorbing material is within that region as well, perhaps in the molecular torus, as has been suggested for Seyfert 2 galaxies. If this obscuration is inside the AGN, then it would affect Hβ but not [O III], which can explain why the [O III] $\lambda 5007$/Hβ ratio of 3.4 is higher in IRAS 20181−2244 compared to other NLS1s (Halpern & Moran 1998). Goodrich (1989) also showed that the three NLS1 galaxies in his sample with $P \geq 1\%$ have high [O III] $\lambda 5007$/Hβ ratios.

5. SUMMARY

IRAS 20181−2244 is a luminous optical and X-ray source. The presence of Fe II emission lines in our spectrum confirms the Halpern & Moran (1998) conclusion that it is a luminous narrow-line Seyfert 1 rather than a type 2 QSO.

Imaging polarimetry and spectropolarimetry measurements indicate it is polarized at about 2.3% ± 0.09% at $\theta = 127°$ after a correction for interstellar polarization in our Galaxy. P and θ are constant with wavelength, which is similar to I Zw 1 but is not common for NLS1s, which more often show P rising to the blue, probably indicative of dust reflection. Spectropolarimetry indicates that the scattering material is inside the BLR. The Balmer lines are visible in the polarized flux, but do not show evidence of an obscured BLR, consistent with the object not being a type 2 QSO. Although several other X-ray–selected targets have not survived their designation as type 2 QSOs (see, e.g., Forster & Halpern 1996; Halpern, Eracleous, & Forster 1998), *ASCA* detections are being made of some of the ultraluminous *IRAS* galaxies that have QSO luminosities, broad Balmer lines in polarized flux (or broad Paschen lines in the infrared), and can be labeled type 2 QSOs (Brandt et al. 1997; Ogasaka et al. 1997).

IRAS 13224−3809 is a well-studied X-ray source and is unusual for its variability at X-ray and UV wavelengths. Our single measurement suggests it is not polarized above what is consistent with a Galactic interstellar polarization. In view of the results of Smith et al. (1997) on the polarization variability of I Zw 1, polarimetric monitoring of these objects, especially IRAS 20181−2244, could be informative.

REFERENCES

Antonucci, R. R. J. 1983, Nature, 303, 158
Antonucci, R. R. J., & Miller, J. S. 1985, ApJ, 297, 621
Boller, T., Brandt, W. N., Fabian, A. C., & Fink, H. H. 1997, MNRAS, 289, 393
Boller, T., Meurs, E. J. A., Brinkman, W., Fink, H., Zimmerman, U., & Adorf, H. M. 1992, A&A, 262, 57
Boller, T., Trumper, J., Molendi, S., Fink, H., Schaeidt, S., Caulet, A., & Dennefeld, M. 1993, A&A, 279, 53
Brandt, W. N., Fabian, A. C., Takashashi, K., Fujimoto, R., Yamashita, A., Inoue, H., & Ogasaka, Y. 1997, MNRAS, 290, 617
Breeveld, A. A., & Puchnarewicz, E. M. 1998, MNRAS, 295, 568
Brindle, C., Hough, J. H., Bailey, J. A., Axon, D. J., Ward, M. J., Sparks, W. B., & McClean, I. S. 1990, MNRAS, 244, 577
Condon, J. J., Cotton, W. D., Greisen, E. W., Yin, Q. F., Perley, R. A., Taylor, G. B., & Broderick, J. J. 1998, AJ, 115, 1693
Elizalde, F., & Steiner, J. E. 1994, MNRAS, 268, L47
Forster, K., & Halpern, J. P. 1996, ApJ, 468, 565
Frecker, J., & Serkowski, K. 1974, Appl. Opt., 15, 605
Goodrich, R. W. 1989, ApJ, 342, 224
———. 1991, PASP, 103, 1314
Goodrich, R. W., & Miller, J. S. 1994, ApJ, 434, 82
Grupe, D., Wills, B. J., Wills, D., & Beuermann, K. 1998, A&A, 333, 827
Halpern, J. P., Eracleous, M., & Forster, K. 1998, ApJ, 501, 103
Halpern, J. P., & Moran, E. C. 1998, ApJ, 494, 194
Heisler, C. A., Lumsden, S. L., & Bailey, J. A. 1997, Nature, 385, 700
Kay, L. E., Antonucci, R., & Coleman, P. 1992, BAAS, 24, 1173
Kay, L. E., & Moran, E. C. 1998, PASP, 110, 1003
Leighly, K. M. 1999, ApJS submitted
Leighly, K. M., Kay, L. E., Wills, B. J., Wills, D., & Grupe, D. 1997, ApJ, 489, L137

Leighly, K. M., Mushotzky, R. F., Yaqoob, T., Kuneida, H., & Edelson, R. 1996, ApJ, 469, 147
Magalhães, A. M., Benedetti, E., & Roland, E. 1984, PASP, 96, 384
Magalhães, A. M., Rodrigues, C. V., Margoniner, V. E., Pereyra, A., & Heathcote, S. 1996, in ASP Conf. Ser. 97, Polarimetry of the Interstellar Medium, ed. D. C. B. Whittet & W. Roberge (San Francisco: ASP), 118
Martel, A. 1996, Ph.D. thesis, Univ. California, Santa Cruz
Mathewson, D. S., & Ford, V. L. 1970, MmRAS, 74, 139
Miller, J. S., & Goodrich, R. W. 1990, ApJ, 355, 456
Miller, J. S., Robinson, L. B., & Goodrich, R. W. 1988, in Instrumentation for Ground-based Astronomy, ed. L. B. Robinson (New York: Springer), 157
Moran, E. C., Helfand, D. J., & Halpern, J. 1996, ApJS, 106, 341
Ogasaka, Y., Inoue, H., Brandt, W. N., Fabian, A. C., Kii, T., Nakagawa, T., Fujimoto, R., & Otani, C. 1997, PASJ, 49, 179
Osterbrock, D. E., & Pogge, R. W. 1985, ApJ, 297, 166
Phillips, M. M. 1976, ApJ, 208, 37
Puchnarewicz, E. M., Mason, K. O., Córdova, F. A., Kartje, J., Branduardi-Raymont, G., Mittaz, J. P. D., Murdin, P. G., & Allington-Smith, J. 1992, MNRAS, 256, 589
Puchnarewicz, E. M., Mason, K. O., Siemiginowska, A., & Pounds, K. A. 1995, MNRAS, 276, 20
Schlegel, D. J., Finkbeiner, D. P., & Davis, M. 1998, ApJ, 500, 525
Serkowski, K. 1974, in Methods of Experimental Physics, Vol. 12, Part A, ed. M. L. Meeks & N. P. Carleton (New York: Academic), 361
Serkowski, K., Mathewson, D. S., & Ford, V. L. 1975, ApJ, 196, 261
Smith, P., Schmidt, G. D., Allen, R. G., & Hines, D. 1997, ApJ, 488, 202
Stark, A. A., Gammie, C. F., Wilson, R. W., Bally, J., Linke, R. A., Heiles, C., & Hurwitz, M. 1992, ApJS, 79, 77
Stephens, S. A. 1989, AJ, 97, 10

Tinbergen, J., & Rutten, R. 1992, A Users Guide to WHT Spectro-
    polarimetry
Tran, H., Cohen, M., & Goodrich, R. 1995, AJ, 110, 2597
Turnshek, D. A., Bohlin, R. C., Williamson, R. L., II, Lupie, O. L., Koorn-
    neef, J., & Morgan, D. H. 1990, AJ, 99, 1243

Ulvestad, J. S, Antonucci, R. R. J., & Goodrich, R. W. 1995, AJ, 109, 81
Wills, B. J., Wills, D., Evans, N. J., Natta, A., Thompson, K. L., Breger, M.,
    & Sitko, M. L. 1992, ApJ, 409, 96
Young, S., Hough, J. H., Efstathiou, A., Wills, B. J, Bailey, J. A., Ward,
    M. J., & Axon, D. J. 1996, MNRAS, 281, 1206